

Exact Symbol Error Probability Analysis of Orthogonal Space-Time Block Codes over Correlated Fading Channels

Mohammad Gharavi-Alkhansari
University of Duisburg-Essen
Dept. of Communication Systems
BA 253, Bismarckstr. 81
D-47057, Duisburg
Germany
gharavi@sent5.uni-duisburg.de

Alex B. Gershman¹
McMaster University
Dept. of ECE
1280 Main St. W., Hamilton
Ontario, L8S 4K1
Canada
gershman@ieee.org

Martin Haardt
Ilmenau University of Technology
Communications Research Lab.
P.O. Box 100565
D-98684, Ilmenau
Germany
haardt@ieee.org

Abstract — Exact expressions for the symbol error probability at the output of the maximum likelihood (ML) decoder are obtained for multiple-input multiple-output (MIMO) systems coded by orthogonal space-time block codes (OSTBCs) over correlated fading channels. Such expressions are derived for the general case of arbitrary input signal constellations and OSTBC, as well as arbitrary correlations of Rayleigh/Rician fading channel coefficients.

I. INTRODUCTION

Orthogonal space-time block codes (OSTBCs) [1], [2] have been a topic of growing interest because they enjoy high performance and offer simple maximum likelihood (ML) decoding.

Recently, several attempts to analyze the error probability of OSTBCs have been made for the coherent receiver case where the channel state information is known at the decoder [3], [4], [5], [6], [7]. However, the results of these papers are limited by the case of uncorrelated Rayleigh fading channel, and the error probability analysis in [3], [4], [5], [6], and [7] is either approximate or is restricted because of assuming some specific class of input signal constellations. For example, an approximate expression for the probability of error of any space-time code in the BPSK case was obtained in [3], while an upper bound on the pairwise symbol error probability of OSTBCs was found in [4]. In [5], an approximate expression was derived for the bit error rate (BER) of OSTBCs that use the M-PSK modulation. Exact BER results were obtained in [6], but these results are limited to the Alamouti code and M-PSK modulation. Exact expressions for the symbol error probability of an arbitrary OSTBC were derived in [7], but the analysis in this paper is applicable to the M-PSK and M-QAM input constellations only.

Recently, an exact and more general analysis of the symbol error probability of OSTBCs has been reported in [8] and [9]. The results of [8] and [9] apply both to the Rayleigh and Rician uncorrelated channel cases, and to the general case of an arbitrary OSTBC and arbitrary input constellation of each symbol. However, these results cannot be directly applied to the correlated channel case.

¹The work of A. B. Gershman has been supported by the Natural Sciences and Engineering Research Council (NSERC) of Canada; Communications and Information Technology Ontario (CITO); Premier's Research Excellence Award Program of the Ministry of Energy, Science, and Technology (MEST) of Ontario; and Wolfgang Paul Award Program of the Alexander von Humboldt Foundation.

An interesting contribution to the OSTBC error probability analysis in the correlated channel case has been recently reported in [10]. However, the analysis presented in this work is restricted to the Rayleigh channel case and the pairwise error probability (or, equivalently, BPSK input constellation) only. Also, the authors of [10] have limited their consideration to a particular channel model which assumes independent transmit and receive antenna correlations [11].

In this letter, we extend the results of [8] and [9] to the correlated channel case. In contrast to [10], our error probability analysis is exact and applies to the general case of arbitrary input constellations, arbitrary channel correlations, and both to the Rayleigh and Rician channel cases.

II. OSTBC BACKGROUND

The input-output relationship for a MIMO system with N transmit and M receive antennas and flat block-fading channel can be expressed as

$$\mathbf{y}(t) = \mathbf{x}(t)\mathbf{H} + \mathbf{v}(t) \quad (1)$$

where \mathbf{H} is the $N \times M$ complex channel matrix, and

$$\begin{aligned} \mathbf{y}(t) &= [y_1(t) \ y_2(t) \ \cdots \ y_M(t)] \\ \mathbf{x}(t) &= [x_1(t) \ x_2(t) \ \cdots \ x_N(t)] \\ \mathbf{v}(t) &= [v_1(t) \ v_2(t) \ \cdots \ v_M(t)] \end{aligned}$$

are the complex row vectors of the received signals, transmitted signals, and noise, respectively.

Assuming that the channel is used at times $t = 1, 2, \dots, T$, and \mathbf{H} does not change during this period, we can rewrite (1) as

$$\mathbf{Y} = \mathbf{X}\mathbf{H} + \mathbf{V} \quad (2)$$

where \mathbf{Y} is the $T \times M$ complex matrix of the received signals, \mathbf{X} is the $T \times N$ complex matrix of the transmitted signals, and \mathbf{V} is the $T \times M$ complex matrix of zero-mean independent identically distributed (i.i.d.) Gaussian noise with the variance σ^2 per real dimension.

Let us denote the complex information-bearing symbols prior to space-time encoding as s_1, \dots, s_K and define the vector

$$\mathbf{s} \triangleq [s_1 \ s_2 \ \cdots \ s_K]^T$$

where $(\cdot)^T$ stands for the transpose. If an OSTBC is used, then the matrix $\mathbf{X} = \mathbf{X}(\mathbf{s})$ in (2) has the following properties [2]:

- all the elements of $\mathbf{X}(\mathbf{s})$ are linear functions of s_1, s_2, \dots, s_K and their complex conjugates;

- $\mathbf{X}^H(\mathbf{s})\mathbf{X}(\mathbf{s}) = \|\mathbf{s}\|_2^2 \mathbf{I}_N$ for all $\mathbf{s} \in \mathbb{C}^K$ where $\|\cdot\|_2$ denotes the Euclidean norm, $(\cdot)^H$ denotes the Hermitian transpose, and \mathbf{I}_N is the $N \times N$ identity matrix.

Let us assume that each information symbol s_k is drawn from a possibly different constellation given by the set

$$\mathcal{U}_k = \{u_{1,k}, u_{2,k}, \dots, u_{I_k,k}\}$$

of cardinality I_k , where each member of the set \mathcal{U}_k belongs to the complex plane \mathbb{C} . In turn, the selected complex vector \mathbf{s} is a member of the constellation set

$$\mathcal{S} \triangleq \{\mathbf{s}_1, \mathbf{s}_2, \dots, \mathbf{s}_L\} = \mathcal{U}_1 \times \mathcal{U}_2 \times \dots \times \mathcal{U}_K$$

where

$$L \triangleq \prod_{k=1}^K I_k.$$

The OSTBC is then applied to the complex vector \mathbf{s} to form the $T \times N$ matrix $\mathbf{X}(\mathbf{s})$. The space-time coded signal \mathbf{X} belongs to a constellation

$$\mathcal{X} \triangleq \{\mathbf{X}_1, \mathbf{X}_2, \dots, \mathbf{X}_L\}$$

where

$$\mathbf{X}_\ell = \mathbf{X}(\mathbf{s}_\ell), \quad \ell = 1, 2, \dots, L.$$

We consider the case when the coherent ML decoder is used, i.e., \mathbf{H} is known at the receiver. The constellation of the received symbols is given by

$$\mathcal{Y} = \{\mathbf{Y}_1, \mathbf{Y}_2, \dots, \mathbf{Y}_L\}$$

where

$$\mathbf{Y}_\ell = \mathbf{X}_\ell \mathbf{H}.$$

The task of the ML decoder is to find

$$\ell_{\text{opt}} = \underset{\ell \in \{1, \dots, L\}}{\text{argmin}} \|\mathbf{Y} - \mathbf{Y}_\ell\|_F$$

where $\|\cdot\|_F$ denotes the Frobenius norm.

In [12], [13], and [14], it has been shown that the ML decoder for an OSTBC modulated signal is made up of a linear combiner followed by a quantizer, and the K complex outputs of the linear combiner, denoted by w_k , $k = 1, 2, \dots, K$, can be written as

$$w_k = \|\mathbf{H}\|_F s_k + \xi_k, \quad k = 1, 2, \dots, K \quad (3)$$

where ξ_k are i.i.d. complex Gaussian variables with variance σ^2 per real dimension. This shows that the effective channel from before the OSTBC encoding to after the linear combiner is equivalent to K parallel single-input single-output (SISO) additive white Gaussian noise channels. This property is sometimes called the SISO equivalency of the OSTBC.

If we use the notations

$$\begin{aligned} \mathbf{w} &\triangleq [w_1, w_2, \dots, w_K]^T \\ \boldsymbol{\xi} &\triangleq [\xi_1, \xi_2, \dots, \xi_K]^T \end{aligned}$$

then (3) may be rewritten as

$$\mathbf{w} = \|\mathbf{H}\|_F \mathbf{s} + \boldsymbol{\xi}. \quad (4)$$

We will denote the constellation of \mathbf{w} by \mathcal{W} . Equation (4) implies that the combined effect of the OSTBC, the channel and the linear processing at the ML receiver on the input constellation \mathcal{S} is equivalent to a uniform scaling of \mathcal{S} by the factor of

$\|\mathbf{H}\|_F$, and that the shapes of the constellations \mathcal{W} and \mathcal{S} are the same except for a scaling factor.

Equation (4) follows more intuitively from a stronger *constellation invariance property* of OSTBCs [8], which says that for any OSTBC, the constellation invariance not only exists between \mathcal{S} and \mathcal{W} , but also between \mathcal{S} , \mathcal{X} , and \mathcal{Y} in the sense that \mathcal{X} and \mathcal{Y} have exactly the same “shape” as \mathcal{S} except for scaling factors of \sqrt{N} and $\|\mathbf{H}\|_F$, respectively. In contrast to the invariance implied by the SISO equivalency of the OSTBC, the constellation invariance is not related to the type of decoder used. This property is due to the fact that the OSTBC positions the transmitted signal constellation in a certain subspace of the inner product space of complex $N \times T$ matrices that is immune to the skewing effects of the channel.

In the case of fixed \mathbf{H} , let us denote the error probability of decoding the symbol s_k by the coherent ML decoder as $P(\mathcal{E}_k|\mathbf{H})$. In the case of random \mathbf{H} , let this error probability averaged over realizations of \mathbf{H} be denoted as $P(\mathcal{E}_k) \triangleq E\{P(\mathcal{E}_k|\mathbf{H})\}$, where $E\{\cdot\}$ is the statistical expectation operator. In [8] and [9], (4) has been used to show that

$$P(\mathcal{E}_k) = 1 - \frac{1}{I_k} \sum_{i=1}^{I_k} \iint_{R_{i,k}} p_{X,Y}(x - \text{Re}(u_{i,k}), y - \text{Im}(u_{i,k})) dx dy \quad (5)$$

where $Z \triangleq \|\mathbf{H}\|_F^2$, $p_Z(z)$ is the pdf of Z , $R_{i,k}$ is the optimal decision region for $u_{i,k}$ in \mathbb{C} , and

$$p_{X,Y}(x, y) = \int_0^\infty \frac{z}{2\pi\sigma^2} \exp\left(-z \frac{x^2 + y^2}{2\sigma^2}\right) p_Z(z) dz \quad (6)$$

is the “effective” pdf of the noise. In the uncorrelated channel case, the real and imaginary parts of the elements of \mathbf{H} are all independent Gaussian random variables with the same variance and Z has a chi-square distribution. In this case, the pdf $p_Z(z)$ has a closed-form expression. In [8] and [9], this expression was substituted in (6) and then the resulting integral was evaluated to obtain $p_{X,Y}(x, y)$. However, in the general case when the elements of \mathbf{H} are correlated Gaussian random variables, the pdf of Z does not have any closed form [15, Chapter 29], and the method of [8] and [9] cannot be applied to compute $P(\mathcal{E}_k)$.

III. ERROR PROBABILITY ANALYSIS FOR CORRELATED MIMO CHANNELS

In this section, we will use a moment generating function (MGF) based technique² to extend the results of [8] and [9] to the correlated channel case and to compute $P(\mathcal{E}_k)$ explicitly. Using the notations

$$a \triangleq \frac{1}{2\pi\sigma^2}, \quad b \triangleq -\frac{x^2 + y^2}{2\sigma^2} \quad (7)$$

equation (6) can be written in the following form

$$p_{X,Y}(x, y) = a \int_0^\infty z e^{bz} p_Z(z) dz. \quad (8)$$

If we denote the MGF of Z as $M(t)$, and its derivative as $M'(t)$, then

$$\begin{aligned} M(t) &\triangleq E\{e^{Zt}\} = \int_0^\infty e^{zt} p_Z(z) dz \\ M'(t) &= E\{Z e^{Zt}\} = \int_0^\infty z e^{zt} p_Z(z) dz. \end{aligned} \quad (9)$$

²Note that MGF-related techniques have found numerous applications to error probability analysis of fading single-input single-output (SISO) and single-input multiple-output (SIMO) channels, see [16] and references therein.

Using (9), equation (8) can be written as

$$p_{X,Y}(x,y) = aM'(b). \quad (10)$$

Fortunately, simple closed-form expressions can be obtained for the MGF of Z .

Let us introduce the ‘‘underline’’ operator that for any $I \times P$ complex matrix \mathbf{A} is defined as

$$\underline{\mathbf{A}} \triangleq \begin{bmatrix} \text{vec}\{\text{Re}(\mathbf{A})\} \\ \text{vec}\{\text{Im}(\mathbf{A})\} \end{bmatrix} \quad (11)$$

where $\text{vec}\{\cdot\}$ is the vectorization operator stacking all columns of a matrix on top of each other. Note that $\underline{\mathbf{A}}$ is a $2PI \times 1$ real vector.

The covariance matrix of $\underline{\mathbf{H}}$ is given by

$$\mathbf{C} \triangleq \text{E}\{(\underline{\mathbf{H}} - \text{E}\{\underline{\mathbf{H}}\})(\underline{\mathbf{H}} - \text{E}\{\underline{\mathbf{H}}\})^T\}.$$

Using the eigendecomposition of \mathbf{C} , we can write

$$\mathbf{C} = \mathbf{U}\mathbf{\Lambda}\mathbf{U}^T \quad (12)$$

where

$$\mathbf{\Lambda} = \text{diag}\{\rho_1^2, \dots, \rho_{2MN}^2\}$$

is the diagonal matrix of the eigenvalues ρ_i^2 ($i = 1, \dots, 2MN$) of \mathbf{C} , and \mathbf{U} is the $2MN \times 2MN$ real unitary matrix of its corresponding eigenvectors. Note that \mathbf{C} is symmetric and positive semi-definite and, therefore, all its eigenvalues are non-negative. If we use the notation

$$\underline{\mathbf{H}} \triangleq \mathbf{U}^T \mathbf{H} \triangleq [W_1, W_2, \dots, W_{2MN}]^T$$

then it is easy to show that W_i ($i = 1, 2, \dots, 2MN$) are all independent Gaussian random variables with the variances ρ_i^2 ($i = 1, 2, \dots, 2MN$), respectively. If we denote the mean of W_i by μ_i , then

$$[\mu_1, \mu_2, \dots, \mu_{2MN}]^T = \mathbf{U}^T \text{E}\{\underline{\mathbf{H}}\}. \quad (13)$$

It is clear that

$$Z = \|\mathbf{H}\|_F^2 = \|\underline{\mathbf{H}}\|_2^2 = \|\hat{\underline{\mathbf{H}}}\|_2^2 = \sum_{i=1}^{2MN} W_i^2.$$

As all W_i^2 are independent, the MGF of Z is the product of the MGFs of W_i^2 . The random variables W_i^2 have a noncentral chi-squared distribution with one degree of freedom whose MGF is known to be [15]

$$(1 - 2t\rho_i^2)^{-1/2} \exp\left(\frac{t\mu_i^2}{1 - 2t\rho_i^2}\right).$$

Therefore, the MGF of Z and its derivative become

$$M(t) = \prod_{i=1}^{2MN} \left((1 - 2t\rho_i^2)^{-1/2} \exp\left(\frac{t\mu_i^2}{1 - 2t\rho_i^2}\right) \right) \quad (14)$$

$$M'(t) = \left(\sum_{i=1}^{2MN} \frac{\rho_i^2 (1 - 2t\rho_i^2) + \mu_i^2}{(1 - 2t\rho_i^2)^2} \right) \times \left(\prod_{i=1}^{2MN} (1 - 2t\rho_i^2)^{-1/2} \exp\left(\frac{t\mu_i^2}{1 - 2t\rho_i^2}\right) \right). \quad (15)$$

respectively. Substituting (7) and (15) into (10) yields

$$p_{X,Y}(x,y) = \frac{1}{2\pi} \left(\sum_{i=1}^{2MN} \frac{\frac{\rho_i^2}{\sigma^2} \left(1 + (x^2 + y^2) \frac{\rho_i^2}{\sigma^2}\right) + \frac{\mu_i^2}{\sigma^2}}{\left(1 + (x^2 + y^2) \frac{\rho_i^2}{\sigma^2}\right)^2} \right) \times \prod_{i=1}^{2MN} \left(\left(1 + (x^2 + y^2) \frac{\rho_i^2}{\sigma^2}\right)^{-1/2} \exp\left(-\frac{\frac{1}{2}(x^2 + y^2) \frac{\mu_i^2}{\sigma^2}}{1 + (x^2 + y^2) \frac{\rho_i^2}{\sigma^2}}\right) \right). \quad (16)$$

Equations (5) and (16) express the probability of error in the case of an arbitrary correlated Rician channel in a closed form. Note that, according to (12), the channel correlation properties are determined in (16) by the values of ρ_i^2 ($i = 1, \dots, 2MN$). In particular, if $\rho_1^2 = \rho_2^2 = \dots = \rho_{2MN}^2 \triangleq \rho^2$, then the channel is uncorrelated with the covariance matrix $\mathbf{C} = \rho^2 \mathbf{I}_{2MN}$.

There are several interesting observations that can be made from (5) and (16). If the parameter MN is fixed, then the symbol error probability does not depend on specific values of M and N (this property shows a certain reciprocity between the transmitter and the receiver). Also, if MN and input constellations $\{\mathcal{U}_k\}_{k=1}^K$ are all given, then the symbol error probability is independent of the particular choice of OSTBC.

In the special case of uncorrelated channel ($\rho_1 = \rho_2 = \dots = \rho_{2MN} \triangleq \rho$), equation (16) reduces to

$$p_{X,Y}(x,y) = \frac{\frac{\rho^2}{\sigma^2} \left(\frac{\lambda/2}{\frac{\rho^2}{\sigma^2}(x^2 + y^2)^2 + 1} + MN \right)}{\pi \left(\frac{\rho^2}{\sigma^2}(x^2 + y^2)^2 + 1 \right)^{MN+1}} \times \exp\left(-\frac{\lambda}{2} \frac{\frac{\rho^2}{\sigma^2}(x^2 + y^2)^2}{\frac{\rho^2}{\sigma^2}(x^2 + y^2)^2 + 1}\right) \quad (17)$$

where

$$\lambda \triangleq \|\text{E}\{\mathbf{H}\}\|_F^2 / \rho^2.$$

Equation (17) coincides with (24) of [8].

In the case of correlated Rayleigh fading channel, we have $\mu_i = 0$ ($i = 1, 2, \dots, 2MN$), and (16) can be simplified to

$$p_{X,Y}(x,y) = \frac{1}{2\pi} \left(\sum_{i=1}^{2MN} \frac{\frac{\rho_i^2}{\sigma^2}}{\left(1 + (x^2 + y^2) \frac{\rho_i^2}{\sigma^2}\right)} \right) \times \prod_{i=1}^{2MN} \left(1 + (x^2 + y^2) \frac{\rho_i^2}{\sigma^2}\right)^{-1/2}. \quad (18)$$

In the next section, our theoretical results (16) and (18) will be compared with simulation results.

IV. COMPARISON OF THEORETICAL AND SIMULATION RESULTS

In order to see the effect of the channel correlation on the effective pdf of the noise for a Rayleigh channel, Fig. 1 shows the one-dimensional slice of $p_{X,Y}(x,y)$ evaluated using (18) and by simulations at $y = 0$ for different correlation levels. In this figure, we assumed

$$\begin{aligned} M &= N = 4 \\ \sigma^2 &= 1 \\ \rho_i^2 &= \begin{cases} \eta/J, & i = 1, \dots, J \\ 0, & i = J + 1, \dots, 2MN \end{cases} \\ \eta &= 10. \end{aligned}$$

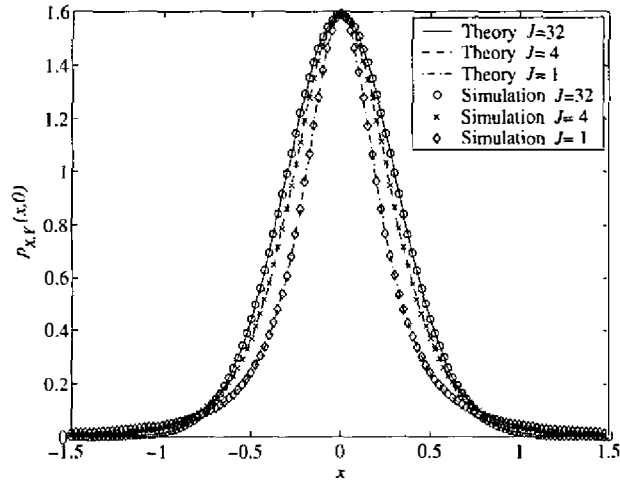


Figure 1: $p_{X,Y}(x,0)$ for different values of J in the Rayleigh fading channel case. Smaller J correspond to more correlated channel.

Here, J is the rank of \mathbf{C} and the parameter η characterizes the strength of the channel. Low values of J correspond to a highly correlated channel (whose covariance matrix is low rank), while higher values of this parameter correspond to a less correlated channel, so that at the maximal value of J , $J_{\max} = 2MN = 32$, the channel becomes uncorrelated. The simulation points in Fig. 1 are obtained using the half-rate code of [2], the QPSK input constellation with the minimum distance of $\sqrt{2}$, and 4×10^8 symbols transmitted. This figure shows fine agreement of the theoretical and simulation points. It also demonstrates that increasing the correlation of the noise (while making the central part of this pdf narrower). This explains qualitatively why channel correlation leads to higher symbol error rates (SERs).

Fig. 2 shows the SER versus the correlation (in terms of J) for the same example as before and for different values of η . For each simulation point in Fig. 2, symbols were transmitted until at least 2×10^4 symbol errors occurred. Similar to the previous figure, this figure shows fine agreement of the theoretical and simulation results. It can be seen from Fig. 2 that the SER reduces as the channel becomes more and more uncorrelated. This effect is especially pronounced at large values of η .

In the Rician case, the channel matrix is given by the sum of the line-of-sight (LOS) and non-line-of-sight (NLOS) components

$$\mathbf{H} = \mathbf{H}_{\text{LOS}} + \mathbf{H}_{\text{NLOS}}$$

where

$$\mathbf{H}_{\text{LOS}} \triangleq \mathbf{E}\{\mathbf{H}\}$$

and

$$\mathbf{H}_{\text{NLOS}} \triangleq \mathbf{H} - \mathbf{H}_{\text{LOS}}.$$

A commonly used yet specific model for correlated Rician fading channels [10, 11] assumes independent transmit and receive correlation matrices. According to this model,

$$\mathbf{H}_{\text{NLOS}} = \mathbf{R}_T^{1/2} \mathbf{H}_w \mathbf{R}_R^{1/2}$$

where \mathbf{R}_R is the $M \times M$ correlation matrix of the receive antennas, \mathbf{R}_T is the $N \times N$ correlation matrix of the transmit

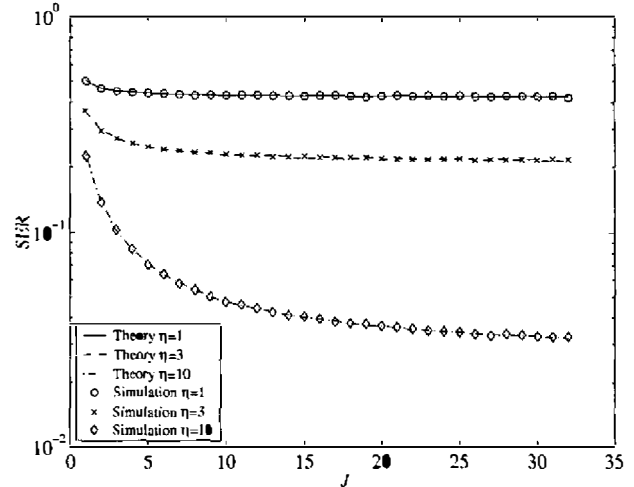


Figure 2: SER versus channel correlation (in terms of J) for different values of η in the Rayleigh fading channel case.

antennas, and \mathbf{H}_w is a complex $N \times M$ matrix whose elements are zero-mean i.i.d. complex Gaussian random variables.

In our next example, we use this particular channel model. We consider the case of $M = N = 2$ and model \mathbf{H} as

$$\mathbf{H} = c_{\text{LOS}} \begin{bmatrix} 1 & 1 \\ 1 & 1 \end{bmatrix} + c_{\text{NLOS}} \begin{bmatrix} 1 & \zeta_T \\ \zeta_T & 1 \end{bmatrix}^{1/2} \mathbf{H}_w \begin{bmatrix} 1 & \zeta_R \\ \zeta_R & 1 \end{bmatrix}^{1/2}$$

where the constants c_{LOS}^2 and c_{NLOS}^2 characterize the powers of the LOS and NLOS components of \mathbf{H} and jointly determine the SNR and the power ratio α of the LOS and NLOS components, and the parameters ζ_R and ζ_T characterize the receive and transmit correlations, respectively. In this example, the Alamouti code is used and the QPSK input constellation is assumed. Fig. 3 shows the SER versus SNR for different values of α in the case when $\zeta_T = \zeta_R = 0.4$. Fig. 4 shows the SER versus SNR for different values of ζ_T and ζ_R in the case when $\alpha = 1$. Similar to the previous two figures, Figs. 3 and 4 both show fine agreement of the theoretical and the simulation results. From Fig. 3, we see that increasing the LOS component with respect to the NLOS one improves the SER at high SNRs. Fig. 4 shows that if the power ratio between the LOS and NLOS components is fixed, then the correlation of the NLOS part of the channel worsens the SER. This effect is similar to that observed from Fig. 2 in the Rayleigh channel case (where only the NLOS component is present).

V. CONCLUSIONS

Exact expressions for the symbol error probability at the output of the coherent maximum likelihood (ML) decoder have been derived for MIMO wireless systems using orthogonal space-time block codes (OSTBCs) over correlated fading channels. Such expressions are derived for the general case of arbitrary input signal constellations and OSTBC, as well as arbitrary correlations of the Rayleigh or Rician fading channel coefficients. Numerical simulation results show fine agreement with the results of our theoretical analysis.

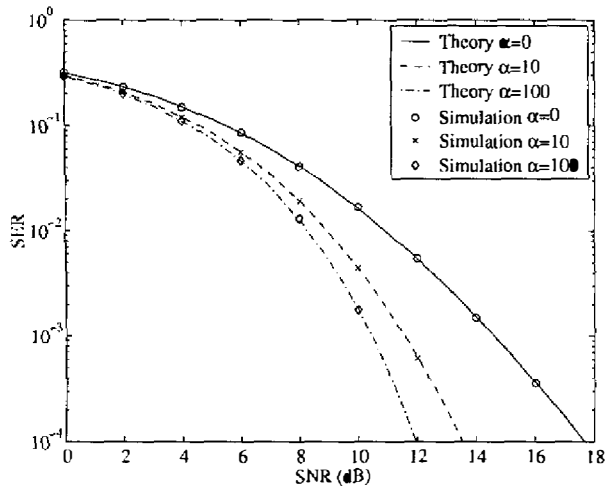


Figure 3: SER versus SNR for different values of α and fixed $\zeta_T = \zeta_R = 0.4$ in the Rician fading channel case.

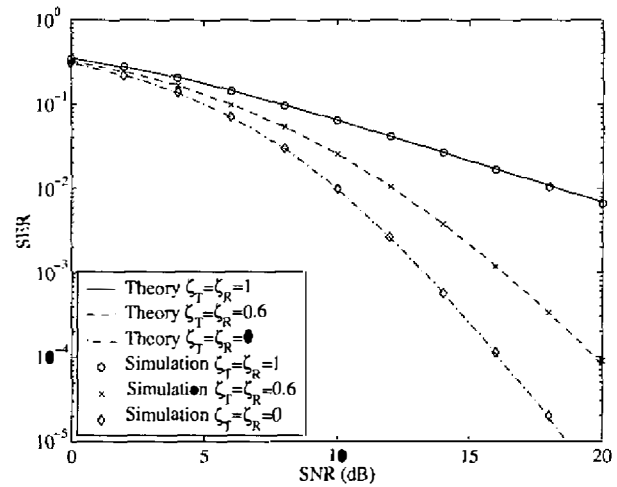


Figure 4: SER versus SNR for different values of ζ_T and ζ_R , and fixed $\alpha = 1$ in the Rician fading channel case.

REFERENCES

- [1] S. M. Alamouti, "A simple transmit diversity technique for wireless communications," *IEEE J. Selected Areas Communications*, vol. 45, pp. 1451-1458, Oct. 1998.
- [2] V. Tarokh, H. Jafarkhani, and A. R. Calderbank, "Space-time block codes from orthogonal designs," *IEEE Trans. Information Theory*, vol. 45, pp. 1456-1467, July 1999.
- [3] G. Ganesan and P. Stoica, "Space-time block codes: A maximum SNR approach," *IEEE Trans. Information Theory*, vol. 47, pp. 1650-1656, May 2001.
- [4] S. Sandhu and A. Paulraj, "Union bound on error probability of linear space-time block codes," in *Proc. IEEE ICASSP*, Salt Lake City, UT, May 2001, pp. 2473-2476.
- [5] G. Bauch and J. Hagenauer, "Analytical evaluation of space-time transmit diversity with FEC-coding," in *Proc. IEEE GLOBECOM*, San Antonio, TX, Nov. 2001, vol. 1, pp. 435-439.
- [6] C. Gao, A. M. Haimovich, and D. Lao, "Bit error probability for space-time block code with coherent and differential detection," in *Proc. IEEE VTC*, Vancouver, BC, Canada, Sept. 2002, vol. 1, pp. 410-414.
- [7] H. Shin and J. H. Lee, "Exact symbol error probability of orthogonal space-time block codes," in *Proc. IEEE GLOBECOM*, Taipei, Taiwan, Nov. 2002, vol. 2, pp. 1197-1201.
- [8] M. Gharavi-Alkhansari and A. B. Gershman, "Constellation space invariance of orthogonal space-time block codes with application to evaluation of the probability of error," in *Proc. IEEE GLOBECOM*, San Francisco, CA, Dec. 2003, vol. 4, pp. 1920-1924.
- [9] —, "Exact symbol error probability analysis for orthogonal space-time block codes: Two- and higher-dimensional constellations cases," to appear in *IEEE Trans. Communications*.
- [10] E. A. Jorswieck and A. Sezgin, "Impact of spatial correlation on the performance of orthogonal space-time block codes," *IEEE Communications Letters*, vol. 8, pp. 21-23, Jan. 2004.
- [11] J. P. Kermaol, L. Schumacher, K. I. Pedersen, P. E. Mogensen, and F. Frederiksen, "A stochastic MIMO radio channel model with experimental validation," *IEEE J. Selected Areas Communications*, vol. 20, pp. 1211-1226, August 2002.
- [12] V. Tarokh, H. Jafarkhani, and A. R. Calderbank, "Space-time block coding for wireless communications: Performance results," *IEEE J. Selected Areas Communications*, vol. 17, pp. 451-460, March 1999.
- [13] S. Sandhu and A. Paulraj, "Space-time block codes: A capacity perspective," *IEEE Communications Letters*, vol. 4, pp. 384-386, Dec. 2000.
- [14] G. Bauch, J. Hagenauer, and N. Seshadri, "Turbo processing in transmit antenna diversity systems," *Annals of Telecommunications*, vol. 56, pp. 455-471, August 2001.
- [15] N. L. Johnson and S. Kotz, *Distributions in Statistics: Continuous Univariate Distributions-2*. Wiley, 1970.
- [16] M. K. Simon and M.-S. Alouini, *Digital Communication over Fading Channels: A Unified Approach to Performance Analysis*. Wiley, 2000.